

Surface Modification of TiO₂ by Phosphate: Effect on Photocatalytic Activity and Mechanism Implication

Dan Zhao,[†] Chuncheng Chen,^{*,†} Yifeng Wang,[†] Hongwei Ji,[†] Wanhong Ma,[†] Ling Zang,[‡] and Jincai Zhao^{*,†}

Beijing National Laboratory for Molecular Sciences, Key Laboratory of Photochemistry, Institute of Chemistry, Chinese Academy of Sciences (CAS), Beijing 100080, China and Department of Chemistry and Biochemistry, Southern Illinois University, Carbondale, Illinois 62901

Received: December 23, 2007; In Final Form: January 29, 2008

Phosphate modified TiO₂ photocatalysts were prepared by phosphoric acid treatment before or after TiO₂ crystallization. Substrates with different structures were chosen to explore the photocatalytic activity of as-modified TiO₂ under UV irradiation. It was found that the effect of phosphate modification is definitely attributed to the surface-bound phosphate anion, and the modification by phosphate can affect both the rates and pathways of photocatalytic reactions, which are of great dependence on the structures and properties of substrates. The degradation of substrates (such as 4-chlorophenol, phenol, and rhodamine B) with weak adsorption on the pure TiO₂ was markedly accelerated by phosphate modification, while substrates (such as dichloroacetic acid, alizarin red, and catechol) with strong adsorption exhibited a much lower degradation rate in the phosphate modified system. A much higher amount of hydroxyl radical was produced in phosphate modified system. All of the experimental results imply that phosphate modification largely accelerates the hydroxyl radical attack, but hinders the direct hole oxidation pathway. A common operating mechanism for the phosphate modification, which can be applicable to other inert anions, is also discussed from the viewpoint of an anion-induced negative electrostatic field in the surface layer of TiO₂ and the hydrogen bond between modification anion and H₂O molecule.

Introduction

TiO₂ semiconductor material is considered to be the most promising heterogeneous photocatalyst for environmental cleanup by solar energy due to its excellent stability and anticorrosion.^{1,2} During the photocatalytic degradation of organic pollutants assisted by TiO₂, an electron in the valence band is excited to the conduction band by ultraviolet light with wavelength shorter than 380 nm, and a positive hole is left in the valence band. The valence band hole can oxidize the hydroxyl group or water adsorbed on the surface of TiO₂ to form the adsorbed or/ and free hydroxyl radical, which is believed to be responsible for the initiation of the degradation reaction.³ Alternatively, the hole is also reported to oxidize the pollutants by direct electron transfer (ET). In most cases, it is difficult to distinguish the two pathways, since they often lead to the generation of same radical species and hydroxylated intermediates. Comparison of these two pathways in photocatalysis is only implicated in a few systems.^{4,5}

The surface modification may have marked influence on the photocatalytic process by altering the charge-transfer pathways occurring at the water–TiO₂ interface. Recently, the modification of TiO₂ by inorganic nonmetal and redox–inert anions (such as F⁻,^{3,6–8} PO₄³⁻,^{9–12} SO₄²⁻,^{13,14} and trifluoroacetic acid¹⁵) has attracted remarkable attention due to their ability in improving the photocatalytic activity of TiO₂. For example, Pelizzetti and co-workers reported that the surface fluorination

of TiO₂ can accelerate the photocatalytic oxidation of phenol.³ Choi et al. also studied the effect of TiO₂ surface fluorination on photocatalytic reactions and photoelectrochemical behaviors.⁶

Phosphate anions are known to adsorb strongly on the surface of TiO₂ by inner-sphere surface complex, which can greatly influence the interfacial and surface chemistry of TiO₂.¹⁶ The earlier studies on the modification of TiO₂ by phosphate and sulfate focused primarily on the improvement of the thermal stability and on the increase of surface area and acid sites on the TiO₂ surface,^{14,17,18} only a few investigations focused on the role of phosphate in the photocatalytic activity of TiO₂, and some rather contradictory results were reported. Matthews et al.¹⁹ reported that the phosphate or sulfate even at millimolar concentrations could reduce the photocatalytic oxidation rates by 20–70%. However, Yu et al.¹¹ recently reported that the phosphate modified TiO₂ exhibited higher photocatalytic activity than pure TiO₂ on oxidation of *n*-pentane in air. They attributed the higher photocatalytic activity of phosphate modified TiO₂ to the extended band gap energy, larger surface area, and the existence of Ti ions in a tetrahedral coordination. Korosi et al.^{9,10} also prepared a series of phosphate modified TiO₂ samples with high surface area, and found that the modified catalysts with a small amount of phosphate could increase the photocatalytic activity for photodegradation of phenol and ethanol. In these works, in order to inhibit the growth of crystallite and increase surface area, the phosphate anion was introduced before the crystallization of TiO₂. Compared with the unmodified TiO₂, photocatalysts modified by this process present so many different properties (such as surface area, the crystallite component and phase, and surface acidity) that it is difficult and complex to reveal the exact role of phosphate anion in the

* To whom correspondence should be addressed. Fax: 86-10-8261-6495. E-mail: jczhao@iccas.ac.cn.

[†] Chinese Academy of Sciences.

[‡] Southern Illinois University.

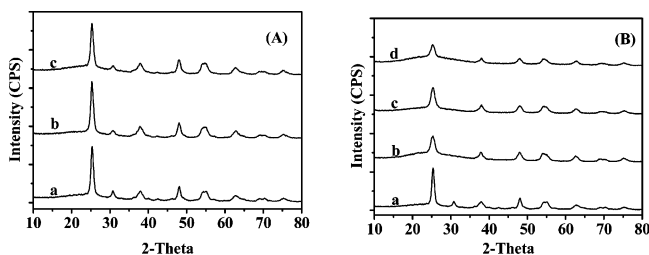


Figure 1. XRD spectra of pure TiO_2 and phosphate modified TiO_2 with several phosphate contents prepared by different methods, (A): (a) pure TiO_2 , (b) $\text{TiO}_2\text{-P1}$, and (c) $\text{TiO}_2\text{-P2}$, (B): (a) TiO_2 (the spectra a in A), (b) P0.05-TiO_2 , (c) P0.10-TiO_2 , and (d) P0.20-TiO_2 .

photocatalysis. As a result, the mechanism for the improvement of photocatalytic activity by phosphate-modification is ambiguous.

In this study, phosphate modification was carried out after the full crystallization of TiO_2 . As expected, the modified TiO_2 holds the same surface area and the crystallite phase as the unmodified one, which simplified the factors that influence the photocatalysis and make it easier to uncover the role of the phosphoric anion in the photocatalytic process. To make clear the effect of surface adsorption on the photodegradation, various substrates with different adsorption ability and anchoring groups on the surface of TiO_2 were chosen. The detailed studies of the intermediates and reactive species were also performed to investigate the effect of phosphate on the photodegradation process. It is found that the phosphate groups bound on the surface of TiO_2 greatly promote the generation of the major reactive radical, $\bullet\text{OH}$ radical, accelerates the hydroxyl radical attack, but hinders the direct hole oxidation pathway. The examination of dechloration, formation of intermediates, changes of TOC and COD during the degradation of 4-chlorophenol shows that more organic intermediates are formed in the phosphate-modified system than in the pure TiO_2 dispersion. The effect of phosphate modification on the photocatalytic activity of TiO_2 should mainly result from the negative electrostatic field in the surface layer of TiO_2 induced by phosphate anions and the activation of H_2O by formation of hydrogen bond between phosphate and H_2O molecule. The results would provide some useful information for the study on photocatalytic mechanism and for design and preparation of efficient TiO_2 -based photocatalysts. In addition, considering that the PO_4^{3-} is commonly present in natural and in the industrial wastewater, and that it was frequently used as a pH buffer in the studies of photocatalysis,^{20,21} the examination of the "adsorption-only effect" of PO_4^{3-} on the photocatalytic degradation of organic pollutants has a helpful implication for the practical application of photocatalysis.

Experimental Section

Materials. Titanium isopropoxide (98%) was purchased from Acros. Rhodamine-B (RhB) dye was of laser-grade quality. Alizarin red (AR), 4-chlorophenol, phenol, hydroquinone, catechol, dichloroacetic acid, isopropyl alcohol, phosphoric acid, and hydrogen peroxide were of analytical reagent grade. Deionized and doubly distilled water was used throughout this study. The pH of the solutions was adjusted with dilute aqueous solutions of HClO_4 and NaOH . It is known that ClO_4^- has low adsorption ability on the surface of metal oxides, and has little effect on the photocatalytic activity of TiO_2 .¹⁹ Accordingly, adjustment of the pH value by HClO_4 can avoid the influence of the anions by competitive adsorption with phosphate anion.

Photocatalyst Preparation. TiO_2 photocatalysts were prepared based on a sol-gel method by alkoxides precursors of

titanium. Titanium isopropoxide (3.0 mL) was dissolved in isopropyl alcohol (20 mL) to obtain a solution of ca. 0.5 M. After ultrasonic mixing, the solution was added dropwise to 20 mL of deionized and doubly distilled water under vigorous stirring. After aging for 2 h, the white gel thus formed was poured into 160 mL water, and stirred for 3 h, then evaporated at 100 °C to remove water. The dry gel was triturated and sintered at 430 °C for 3 h. After having been washed by water thoroughly and dried, pure crystallized TiO_2 was obtained. To load the phosphate ion, the crystallized TiO_2 was soaked in 0.3 M phosphoric acid at 30 °C for 5 h, and then separated by centrifugation. The power was divided into two parts. One was washed thoroughly by water to remove the weak-bound phosphate anion, and dried at 100 °C to obtain $\text{TiO}_2\text{-P1}$. To strengthen the interaction between the phosphate anion and the surface Ti site, the other part was dried directly at 100 °C and further heated at 300 °C for 1.5 h. After having been washed by water thoroughly and dried, the catalyst $\text{TiO}_2\text{-P2}$ was obtained. For comparison, the phosphate modified TiO_2 treated before crystallization was also prepared. The preparing process was the same as that of TiO_2 , except that the aged white gel was poured into, instead of water, 160 mL of phosphoric acid solution with P:Ti ratios of 0.05, 0.10, and 0.20 (denoted P0.05-TiO_2 , P0.10-TiO_2 , and P0.20-TiO_2 , respectively). The gel was then stirred for 3 h, evaporated at 100 °C to remove water, triturated and sintered at 430 °C for 3 h. The sintered catalyst powder was washed by water thoroughly to remove the excess phosphoric acid and dried.

Structural Characterization. X-ray diffraction (XRD) measurements were performed on a Regaku D/Max-2500 diffractometer with the $\text{Cu K}\alpha$ radiation (1.5406 Å). X-ray photoelectron spectroscopy (XPS) data were recorded with an ESCA laboratory 220i-XL spectrometer using $\text{Al K}\alpha$ (1486.6 eV) X-ray source. To eliminate charge effect, all of the spectra were calibrated to the binding energy of adventitious C 1s peak at 284.8 eV. The specific surface areas of the catalysts were measured using 3H-2000III automatic nitrogen sorption BET surface area analyzer. The surface hydroxyl (OH_{ad}) group density of photocatalyst was estimated by thermo gravimetric analysis (TGA). The weight loss of TiO_2 catalysts was monitored by TGA in a thermobalance. The temperature program was as follows: the sample powers were heated in nitrogen from 25 °C to 120 °C at 10 °C/min, held at this temperature for 10 min to remove the physically adsorbed water, and then heated to 650 °C at 20 °C/min. The relative hydroxyl group surface density was calculated using the TGA weight loss and the specific surface area according to reference 32 (eq S1, Supporting Information). The infrared spectra were obtained on a TENSOR 27 FTIR spectrometer (Bruker) in the diffuse reflectance mode, and all samples were dried at 100 °C for 180 min in air before IR experiments. Hitachi U-3010 was used to record the UV-vis diffuse reflectance spectra.

Photodegradation Reaction. The light source used was a 100-W mercury lamp. The 40-mL aqueous solutions containing substrate and pure TiO_2 or phosphate modified TiO_2 catalyst powder were placed in a Pyrex vessel. Prior to irradiation, the suspensions were magnetically stirred in the dark for ca. 30 min to ensure the establishment of an adsorption/desorption equilibrium. At a given time, 3 mL aliquots were collected, centrifuged, and then filtered through a Millipore filter (pore size 0.2 μm) to remove the solid catalyst particles. The filtrate was then subjected to analysis of the concentration and the intermediates using a UV-vis spectrophotometer (Lambda Bio-20) or high-performance liquid chromatography (HPLC) (Di-

TABLE 1: Summary of Physicochemical Properties of Phosphate Modified TiO₂

samples	crystalline size (nm) ^a	SBET (m ² /g) ^b	OH/nm ^{2c}	P/Ti ratio ^d
1 TiO ₂	12.0	85	10.2	0
2 TiO ₂ -P1	11.6	84	9.0	0.09
3 TiO ₂ -P2	11.4	92	8.3	0.18
4 P0.05-TiO ₂	9.0	167	6.2	
5 P0.10-TiO ₂	9.0	187	6.7	0.15
6 P0.20-TiO ₂	9.1	215	6.6	

^a Estimated from broadening of the diffraction peaks by Scherrer formula. ^b BET specific surface area by N₂ adsorption method. ^c Calculated from thermo gravimetric analysis. ^d Determined from the XPS results.

onex P580 pump and UVD340S diode array detector). During HPLC analysis, all intermediates were verified by use of authentic samples. The hydroxyl radical generated was trapped by DMPO and measured using a Bruker model ESP 500 E electron paramagnetic resonance (EPR) spectrometer. The samples for EPR measurements were prepared as follows: a 1.0-mL portion of suspension with 3 mg of pure or phosphate-modified TiO₂ and 80 μL of DMPO (TCI) was exposed to a 100-W mercury lamp under aerated and stirring conditions. A 30-μL portion of suspension was collected at a time interval of 30 s and filled into a quartz capillary for EPR measurements. Total organic carbon (TOC) was assayed by an Apollo 9000 TOC analyzer. Chemical oxygen demand (COD_{Cr}) was measured using the potassium dichromate titration method.

Results and Discussion

Characteristics of Phosphate-Modified Photocatalysts. The status of phosphorus species in the modified TiO₂ catalyst and the influence of phosphate modification on the structure and electronic properties of TiO₂ were intensively investigated first. XRD spectra of the phosphate modified TiO₂ are displayed in Figure 1. It is shown that the crystallite phase for all samples was pure anatase and no other phases (such as rutile) were observed. For the samples treated by phosphoric acid after crystallization (Figure 1A), the XRD patterns exhibited little change with respect to pure TiO₂, and the average crystallite size estimated from the broadening of the diffraction peaks by Scherrer formula was about 11.5 nm (entries 1–3 in Table 1). It indicates that, as expected, this modification process could not influence the crystalline degree and crystallite size of TiO₂. In the cases of phosphoric acid treatment before calcination (Figure 1B and entries 4–6 in Table 1), however, even a small amount of phosphoric acid could lead to a marked broadening of the diffraction peaks (Figure 1B). When the amount of added phosphoric acid corresponded to a P/Ti ratio of 0.05, the size of anatase crystallites decreased from 11.5 to 9.0 nm, and the specific surface area increased from about 85 to 167 m²g⁻¹ (Table 1 entry 4). Further increase in the amount of phosphoric acid tended to present little effect on crystallite size, but resulted in a notable increase in surface areas from 167 to 215 m²g⁻¹ (Table 1 entry 5, 6), suggesting the existence of some amorphous TiO₂ species, which increase with the amount of added H₃PO₄. Evidently, the modifying process by phosphoric acid treatment before crystallization can strongly inhibit the growth of anatase grain and can greatly increase the surface areas of resulting photocatalysts, which is in good agreement with the literature.^{9–11}

The adsorption of phosphate anion on TiO₂ is expected to decrease the density of surface hydroxyl (OH_{ad}).^{6,22} The relative density of the surface hydroxyl group of pure and phosphate-modified TiO₂ was estimated using thermogravimetric analy-

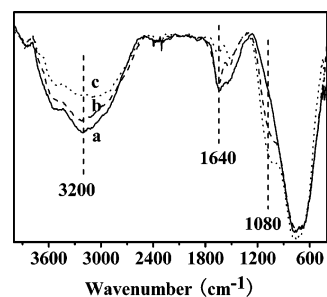


Figure 2. FTIR spectra of pure TiO₂ and phosphate modified TiO₂, (a) TiO₂, (b) TiO₂-P1, and (c) TiO₂-P2.

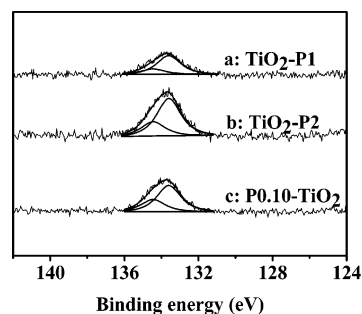


Figure 3. P 2p XPS spectra of phosphate modified TiO₂, (a) TiO₂-P1, (b) TiO₂-P2, and (c) P0.10-TiO₂.

sis.²³ The results are shown in Table 1 and in Figure S1 (Supporting Information). As expected, after the adsorption of phosphate anion, the density of surface hydroxyl group on TiO₂-P1 decreased from 10.2 to 9.0 OH/nm². The density of on TiO₂-P2 OH_{ad} was further reduced. It indicates that the phosphate anion can anchor strongly on the TiO₂ surface by replacing the surface hydroxyl groups. Similarly, for all samples in which the phosphate acid was introduced before the crystallization, low densities of surface hydroxyl were observed (Table 1 entry 4–6).

Figure 2 and Figure S2 (of the Supporting Information) show the FTIR spectra of pure TiO₂ and phosphate modified TiO₂. The strong peak at 750 cm⁻¹ is assigned to the Ti–O–Ti stretching vibration of Ti in a octahedral coordination,²⁴ and the peaks around 3200 (broad) and 1640 cm⁻¹ correspond to the stretching and deformation bands of surface-adsorbed water molecules and hydroxyl groups.^{24,25} After phosphate modification, a new absorption band around 1080 cm⁻¹ appeared on the shoulder of the Ti–O–Ti vibration band, which is the characteristic frequency of the phosphate ions.⁹ In addition, the peak intensity of PO₄³⁻ for TiO₂-P2 (curve c) was stronger than that of TiO₂-P1 (curve b). The bands of surface-adsorbed water molecules and hydroxyl groups (3200 and 1640 cm⁻¹) became weak for TiO₂-P1 relative to the pure TiO₂, and further lessened for the heated sample (TiO₂-P2, curve c), indicating the replacement of OH_{ad} by PO₄³⁻, which confirms the measurement results of the OH_{ad} density. The band of PO₄³⁻ also appeared in the samples modified by phosphate acid before the crystallization, and the intensity became stronger with increase of the added amount of phosphate acid (Figure S2 of the Supporting Information).

XPS was employed to examine the oxidation state and content of PO₄³⁻ on the TiO₂ surface. The P 2p XPS spectra are presented in Figure 3, and the Ti 2p and O 1s spectra are displayed in Figure S3 (of the Supporting Information). P/Ti ratios at the surface of TiO₂ were determined to be 0.09, 0.18, and 0.15 for TiO₂-P1, TiO₂-P2, and P0.10-TiO₂, respectively. All of the phosphate-modified TiO₂ exhibited a binding energy

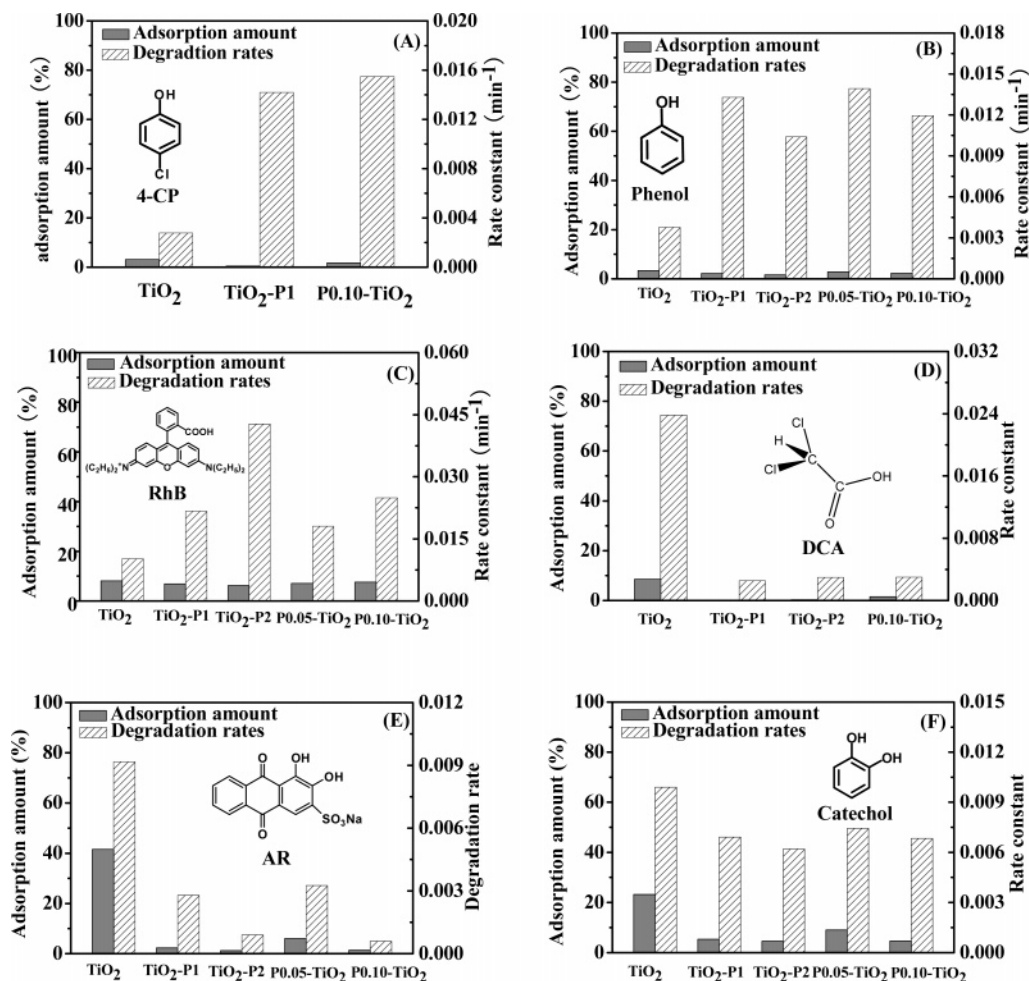


Figure 4. Adsorption and photocatalytic activity of the phosphate modified TiO₂ photocatalysts for the degradation of various substrates in aqueous dispersions under UV irradiation. The adsorption is represented by the adsorption percentage of the added substrates by catalysts under the reaction conditions. (A) 4-chlorophenol (2.0×10^{-4} M, Cat 1.0 g/L, pH = 2.5); (B) phenol (2.0×10^{-4} M, Cat 1.0 g/L, pH = 5.7); (C) Rhodamine B (2.0×10^{-5} M, Cat 0.5 g/L, pH = 2.5); (D) dichloroacetic acid (2.0×10^{-4} M, Cat 1.0 g/L, pH = 3.4); (E) Alizarin red (2.0×10^{-4} M, Cat 0.5 g/L, pH = 4.3); (F) catechol (2.0×10^{-4} M, Cat 1.0 g/L, pH = 2.5).

of P 2p located at around 133.5 eV, indicating that phosphorus in our samples is in pentavalent-oxidation state (P⁵⁺) and presents in the form of P–O bond.²⁶ It is noted that all the P 2p spectra were asymmetric and exhibited a shoulder on the high-energy side, and the spectra can be fitted by two peaks located at 133.6 and 134.5 eV, respectively, and their area ratios for the samples TiO₂-P1, TiO₂-P2, and P0.10-TiO₂ were 0.22, 0.28, and 0.35, respectively. The main peaks at 133.6 eV have a similar binding energy to that of the controlled NaH₂PO₄ (133.9 eV) and Na₂HPO₄ (133.1 eV), which can be assigned to the monodentate coordinated PO₄³⁻ with the surface Ti sites. The heating at 300 °C was expected to strengthen the bond between the phosphate anion and the Ti sites. Also, the binding intensity in P0.10-TiO₂ should be stronger than in that of other samples. In addition, the existence of physically adsorbing phosphate ions had been excluded by thorough washing. The higher area ratios for the peaks at 134.5 eV in samples TiO₂-P2 and P0.10-TiO₂ suggest that the shoulder peaks should be attributed to the phosphate species bonded by bidentate form. It is also noted that the results of XPS, by which the P/Ti ratio (0.15) in the sample P0.10-TiO₂ is much larger than the added phosphoric acid amount (0.10), may be derived from the enrichment of phosphate species on the surface during crystallization. The two Ti 2p_{3/2} peaks (458.8 and 464.5 eV, respectively) in the phosphate-modified samples (Figure S3A curves b–d of the Supporting Information) exhibited little

difference with respect to that of pure TiO₂ (curve a), indicating the Ti is in an octahedral coordination in all of the samples.²⁷ The O 1s XPS spectra had strong peak at 530.0 eV, corresponding to the Ti–O–Ti lattice oxygen of TiO₂. A shoulder at the higher binding energy was also observed, which is assigned to the surface hydroxyl groups (Ti–OH).²⁸ The difference spectra of O 1s between the phosphate-modified and pure TiO₂ (Figure S3C of the Supporting Information) indicate that the O 1s peaks in P–O form (531.2 eV) appeared after the modification, and the change in their intensities are in consistent with the results of FTIR and P/Ti ratios.

Adsorption and Photocatalytic Activity of Phosphate-Modified Photocatalysts. It has been reported that the photocatalytic reaction typically occurs at the surface of photocatalyst. Adsorption of the organic substrates is generally considered to be an important factor in their photocatalytic degradation. The surface occupation by phosphate anions can be competitive with adsorption of organic molecules, and hence influence photocatalytic degradation of the substrates. In this study, therefore, various substrates with different adsorption ability and anchoring groups were chosen. Their relative adsorption amounts and degradation rate constants are displayed in Figure 4, and the corresponding degradation kinetic curves are given in the Supporting Information (Figure S4).

It is shown in Figure 4 that the effect of phosphate modification on TiO₂ is substrate-dependent. The degradations

of 4-chlorophenol (4-CP), phenol, and Rhodamine B (RhB) were accelerated to different extents by the phosphate modification (Figure 4A–C). The adsorption amount of 4-CP (2.0×10^{-4} M initially) in the pure TiO₂ system was only about 3% (corresponding to $6.3 \mu\text{mol/gTiO}_2$). After the modification by PO₄³⁻, the adsorption of 4-CP became much weaker. For example, the adsorption amount on TiO₂-P2 and P0.10-TiO₂ decreased to 0.5% ($0.9 \mu\text{mol/gTiO}_2$) and 1.8% ($3.5 \mu\text{mol/gTiO}_2$), respectively (Figure 4A). For phenol, a similar adsorption tendency on the various catalysts was also observed (Figure 4B). The decay rate constant of 4-CP (fitted by pseudo-first-order process) on pure TiO₂ was $0.0028 \pm 0.0002 \text{ min}^{-1}$. Upon modification with phosphate anion, although the adsorption of 4-CP became weak, the degradation of 4-CP was markedly accelerated, and the kinetic constants increased to $0.014 \pm 0.001 \text{ min}^{-1}$ and $0.015 \pm 0.0004 \text{ min}^{-1}$ for TiO₂-P2 and P0.10-TiO₂, respectively. There was an ~4-fold increase in the rate constants for the degradation of 4-CP in the phosphate modified TiO₂ systems compared to that in the unmodified system. Similarly, the photocatalytic degradation of phenol was also enhanced after phosphate modification (Figure 4B). RhB molecule is zwitterionic. It contains positively charged diethylamine groups and a negatively charged carboxylate group. The carboxylate group is reported to be easily adsorbed to Ti sites on the surface of TiO₂.²⁹ On the other hand, the positively charged diethylamine groups are prone to interact electrostatically with negative species such as phosphate anion adsorbed on TiO₂ surface. On balance, PO₄³⁻ modification of TiO₂ exhibited little effect on the adsorption of RhB. However, its degradation rate was notably accelerated by the PO₄³⁻ modification. The pseudo-first-order rate constant of RhB degradation was promoted from 0.010 min^{-1} for TiO₂ to 0.043 min^{-1} for TiO₂-P2 and 0.025 min^{-1} for P0.10-TiO₂.

In contrast to the cases of 4-CP, phenol, and RhB, the degradations of dichloroacetic acid (DCA), alizarin red (AR), and catechol were greatly suppressed on the phosphate modified TiO₂ (Figure 4D–F). The adsorption of DCA decreased from 8.6% ($17 \mu\text{mol/g TiO}_2$) for TiO₂ to 0.2% for TiO₂-P1, 0.4% for TiO₂-P2 and 1.6% for P0.10-TiO₂. The pseudo-zero-order rate constants for DCA degradation decreased from 0.024 min^{-1} for TiO₂ to 0.0030 min^{-1} for TiO₂-P1 and P0.10-TiO₂, that is, there was about 8-fold of decrease in the degradation of DCA after the phosphate modification. AR also has strong interaction with the surface of TiO₂ through coordination of the two hydroxyls with Ti sites.³⁰ Therefore, TiO₂ exhibited rather strong adsorption for AR, and about 41.6% of AR (2.0×10^{-4} M initial concentration) was adsorbed on TiO₂ ($166 \mu\text{mol/gTiO}_2$). The phosphate modification of TiO₂ markedly suppressed its adsorption. For example, only about 1% of AR was adsorbed in the TiO₂-P2 case. Similar to DCA, the phosphate modification inhibited the degradation of AR. Catechol also possesses of two hydroxyls in ortho positions as AR. Its adsorption and degradation were also lowered in the phosphate modified TiO₂ systems compared with the pure TiO₂.

In our study, the adsorption of all of the substrates, except zwitterionic RhB, was suppressed upon phosphate modification. Phosphate has proven to be a strongly binding anion on the surface of TiO₂. The Langmuir binding constant reported for phosphate onto TiO₂ at pH = 2.3 is $(3.8 \pm 0.8) \times 10^4 \text{ mol}^{-1}\text{L}$, which is similar to the binding constants for bidentate ligand species such as oxalate and catechol.¹⁶ It is evident that the occupancy of the surface Ti sites by phosphate is responsible for the decrease of adsorption of substrates. From Figure 4, it could be found that a common characteristic for the substrates,

for which their degradations were promoted by the phosphate modification, is that their adsorption abilities on the catalyst surface are relatively weak under the experimental conditions. In contrast, all substrates exhibiting suppressive degradation in the PO₄³⁻-modified systems (DCA, AR, and catechol) have a strong adsorption on the pure TiO₂ surface, and their adsorption was markedly suppressed by phosphate modification. In fact, in the photocatalysis of the surface fluorinated TiO₂, Choi and co-workers⁶ also found that both the adsorption and photodegradation rate of DCA markedly decreased in TiO₂-F system and proposed that the photocatalytic degradation of DCA on TiO₂ is mainly initiated by a direct hole oxidation through the formation of bidentate complexes of carboxylate groups with the Ti site. On the basis of detailed kinetic analysis and the time evolution of the intermediates during the photocatalytic transformation of phenol in the presence of different alcohols, Pelizzetti and co-workers⁸ suggested that the oxidation of phenol proceeds 90% through the reaction with TiO₂-bound hydroxyl radicals; the remaining 10% is via direct interaction with the holes. It is well-known that *ortho*-hydroquinone derivatives can anchor to the surface Ti of TiO₂ to form the chelate charge-transfer complex. Their adsorption on TiO₂ is much stronger, and the charge transfer between them and TiO₂ is much easier than that of monohydroxyl phenols such as chlorophenol and phenol. Hoffmann and co-workers⁵ have reported that the direct hole oxidation pathway was more important for strongly adsorbing 4-chlorocatechol, whereas hydroxyl radical attack was more dominated for the poorly adsorbing 4-chlorophenol. Accordingly, our present results imply that phosphate modification largely accelerates the hydroxyl radical oxidation pathway, but hinders the interaction of substrates with TiO₂ and hence suppresses the direct electron-transfer pathway by holes.

In this study, the only possibility for the phosphate groups is to be bound to the surface of TiO₂ crystallites by substituting the surface hydroxyl in TiO₂-P1 and TiO₂-P2 samples, since the TiO₂ is already well-crystallized before the adsorption of phosphate. Moreover, the crystallite size and surface area for phosphate-modified TiO₂ treated after crystallization were found to be unchanged comparing to pure TiO₂. The photodegradation reaction of a series of substrates shows that the phosphate-modified TiO₂ treated after crystallization exhibited similar adsorption and degradation behaviors to the phosphate-modified one treated before crystallization, although the enhanced or suppressed extents were dependent on the synthesis methods and the substrates. It is evident that, in the present study, the changes in the surface area and crystallite structure, resulting from phosphate incorporation into the bulk of crystallite, cannot account for the effect on the photocatalytic properties, as proposed in the earlier work.^{11,12} It should be reasonable to attribute these effects to the surface-bound phosphate anion. Korosi et al.¹⁰ also found that the phosphate modified TiO₂ by sol-gel method lost much of its photocatalytic activity in ethanol oxidation reaction after removing the surface phosphate by treatment with NaHCO₃ solution, which is consistent with our results here.

Intermediate Analysis for Photocatalytic Degradation of 4-Chlorophenol. 4-CP is a kind of poisonous organic pollutant in water. Its photocatalytic degradation has been extensively investigated,^{20,21,31,32} and much mechanistic information has been obtained. In order to make the operating mechanism of phosphate groups in the photocatalytic reaction clearer, the degradation process of 4-CP, including detection of intermedi-

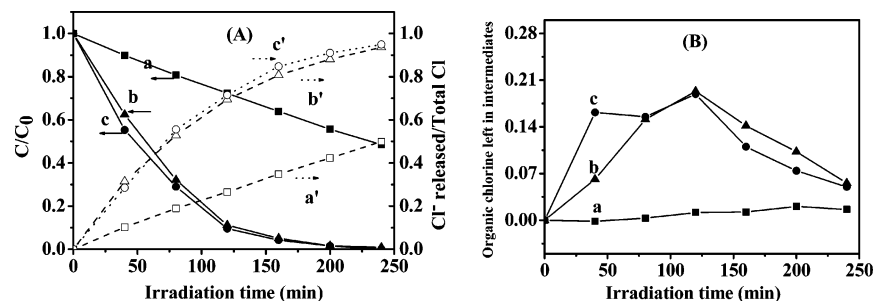


Figure 5. (A) Temporal photocatalytic decay of 4-chlorophenol (black symbols) and release ratio of chloride ion (white symbols) under UV irradiation. (B) The ratio of corresponding organic chlorine left in the degradation intermediates estimated from the chloride ion released and the 4-CP left during the reaction process. (a) TiO₂, (b) TiO₂-P2, and (c) P0.10-TiO₂, 4-CP 2.0×10^{-4} M, Cat 1 g/L, pH = 2.5.

ates and the change of TOC and COD, and the formation kinetics of hydroxyl radical, was examined in more detail in this study.

Figure 5A shows the photocatalytic degradation profiles of 4-CP and the release of chloride ion in the naked TiO₂ and phosphate-modified TiO₂ suspensions under UV irradiation. The chlorine in 4-CP was efficiently removed, along with the degradation in all of the photocatalytic systems. For naked TiO₂, about 50% of 4-CP was degraded and about 50% of chloride ion was released after 240 min of irradiation (curves a and a'). Both degradation and dechlorination rates were significantly promoted by the phosphate modification. Nearly all 4-CP was degraded and about 94% of chlorine was removed in both TiO₂-P2 and P0.10-TiO₂ systems within the same irradiation time (240 min) (curves b, b' and c, c', respectively). It is also noted that the chlorine removal was a little lower than that decay of 4-CP in the phosphate modified systems. By a comparison of the total chlorine added (the initial 4-CP concentration) with the chloride ion released and the 4-CP left in the system, we can estimate the chlorine remained in the organic intermediates during the degradation (Figure 5B). It is found that, in the pure TiO₂ system, there were little chloridized organic intermediates in the whole degradation process (Figure 5B, curve a), indicating that nearly all of the chlorine was transformed to Cl⁻ once the 4-CP was destroyed. By contrast, in the phosphate-modified systems, Cl in the form of Cl⁻ and 4-CP during the photooxidation process was notably less than the total Cl, indicating the formation of chlorine-containing organic intermediates. The maximum Cl concentration in the intermediates (about 20% of the total Cl) appeared at 120 min of irradiation, where about 90% of 4-CP was removed. After that, Cl in the intermediates decreased gradually, indicating the further decomposition of chlorine-containing organic intermediates (Figure 5B, curves b and c).

Hydroquinone and 4-chlorocatechol were reported as the major intermediates in the TiO₂ photocatalytic degradation of 4-CP.^{20,33} In this study, the HPLC method was used to probe the intermediates formed during the photodegradation process. The concentration changes of hydroquinone formed versus the removed percentage of 4-CP in different systems are shown in Figure 6. Only a small quantity of hydroquinone (below 2 μM) was detected in the pure TiO₂ system (curve a). In both the TiO₂-P1 and P0.10-TiO₂ systems, by contrast, a relatively high concentration of hydroquinone was observed (curves b, c). The concentrations of hydroquinone initially increased nearly linearly with the conversion of 4-CP, and the ratios of hydroquinone to the degraded 4-CP was kept about 12.5%, that is, about one hydroquinone was formed from the degradation of eight 4-CP molecules. After the maxima (about 2.6×10^{-5} M), where 90% of 4-CP was degraded, the concentration of hydroquinone underwent a fast drop. The controlled experiment, using the

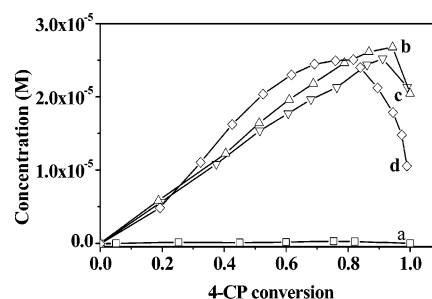


Figure 6. Concentration of hydroquinone versus the conversion of 4-CP in the process of photodegradation assisted by (a) pure TiO₂, (b) P0.10-TiO₂, (c) TiO₂-P2, and (d) photolysis of H₂O₂, 4-CP 2.0×10^{-4} M, Cat 1 g/L, pH = 2.5.

hydroquinone as the initial substrate, showed that the decomposition reaction of hydroquinone was not significantly affected by phosphate modification (Figure S5 of the Supporting Information). Then, the accumulation of hydroquinone in the photodegradation of 4-CP should be ascribed to the acceleration of 4-CP hydroxylation in the phosphate modified suspension. It was also noted that, under the present experimental conditions, about 1 μM of 4-chlorocatechol was observed in both pure TiO₂ and phosphate-modified dispersions, while other chlorine-containing aromatic intermediates were too little to be detected. As shown in Figure 5B, more chlorine-containing organic intermediates formed in the phosphate modified system. Considering the results obtained here, they should be some non-aromatic and acyclic compounds formed by the opening of aromatic ring.

The degradation of 4-CP was also carried out in the presence of UV-irradiated H₂O₂, which is known to form free hydroxyl radical through the photolysis of H₂O₂ by UV irradiation.^{34,35} It was found that the major intermediate detected was also hydroquinone in the UV-H₂O₂ system (Figure 6, curve d). The formation and disappearance tendency of hydroquinone was similar to that in the phosphate modified TiO₂ systems, but very different from that in the pure TiO₂ system. In homogeneous H₂O₂-UV photolytic system, the attack of free hydroxyl radical is expected to be the dominant initial step for the oxidation of 4-CP.³⁵ The similarity in the formation and disappearance tendency of hydroquinone between the phosphate modified TiO₂ and H₂O₂-UV systems implies that the degradation of 4-CP undergoes similar pathway in these two systems, and is also initiated primarily from the free hydroxyl radical attack in the former system. The observation of a lower concentration of aromatic intermediates in the naked TiO₂ dispersion indicates that another pathway besides the hydroxyl radical attack, such as direct electron transfer from 4-CP to hole, may exist to initiate the degradation. In fact, there are many implications that the open ring of aromatics under photocatalytic conditions involves

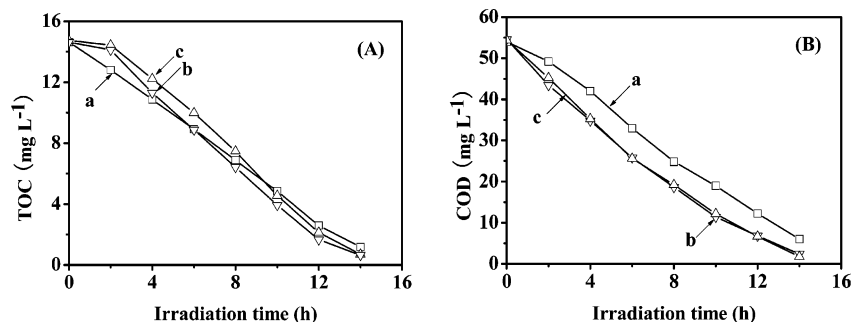


Figure 7. Changes in (A) total organic carbon (TOC) of the degraded bulk solution and (B) chemical oxygen demand (COD_{Ct}) of whole dispersion during the photodegradation of 4-chlorophenol (2×10^{-4} M, 200 mL, pH = 2.5, Cat 200 mg). (a) pure TiO₂, (b) TiO₂-P2, and (c) P0.10-TiO₂.

the hole oxidation.^{20,21,31,35,36} In a study of the comparison between radiolytic and TiO₂-assisted photocatalytic degradation of 4-CP, Kamat and co-workers³¹ showed that when 4-CP is oxidized by hydroxyl radical, significant concentrations of hydroxylated aromatic intermediates such as hydroquinone and 4-chlorocatechol are formed. However, under conditions favoring the direct electron-transfer pathway, such as using azide radicals as electron acceptors, increasing the loading of TiO₂ or increasing the pH value of the dispersion, the degradation of 4-CP produces predominantly nonaromatic intermediates. As shown in Figure 4A, the adsorption of 4-CP was markedly hindered by phosphate modification. The likelihood of direct oxidation should become lower. Accordingly, the relative ratio of hydroxyl radical attack to hole oxidation should increase in the phosphate system. This argument can further rationalize our findings that the formation of aromatic intermediates is more significant in the phosphate modified TiO₂ systems than that in the unmodified one.

The extent of mineralization of 4-CP was examined by determination of both residual total organic carbon (TOC) and chemical oxygen demand (COD). The temporal changes of TOC and COD in the degradation process of 4-CP are shown in Figure 7. In the pure TiO₂ case, the TOC exhibited a linear decrease during the degradation. For the phosphate modified systems, there was a small but significant induction period for the removal of TOC at the initial stage. Repetitious measurements by three runs demonstrate that the presence of the induction period is not attributed to the experimental error. In agreement with our observations, Pelizzetti and co-workers³ also reported the existence of an induction period of TOC removal during the photocatalytic degradation of phenol in the fluoride-modified TiO₂ system. The induction period in the TOC measurement is indicative of the existence of more organic intermediates in the phosphate-modified TiO₂ systems at the early stage of degradation, which is inconsistent with the above observation (Figures 5 and 6). After the induction period, the removal rates of TOC became a little faster in the phosphate systems than that in pure TiO₂ case. However, the overall difference in the removal rate of TOC between the pure and phosphate-modified TiO₂ systems is not as much as that in the disappearance kinetic of 4-CP. For the removal of COD, the decrease rates in the phosphate modified TiO₂ dispersions were greater than that in the pure TiO₂ system during the whole degradation process. COD reflects the oxidation extent of the substrates, while TOC provides the information about mineralization of substrates to CO₂. The formation of organic intermediates by oxidation can decrease COD value of the system, but cannot change TOC value, until the organic intermediates are deeply oxidized to CO₂. Accordingly, the difference in the change tendency between the COD and TOC

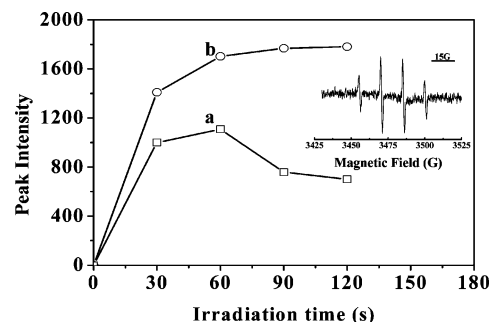


Figure 8. Intensity changes in the EPR signals of DMPO-OH adducts as a function of UV irradiation in (a) pure TiO₂ and (b) phosphate modified TiO₂ (TiO₂-P2) dispersions. Inset: The typical ESR signal of •OH trapped by DMPO (light source 100-W mercury lamp, Cat 3 g/L, DMPO 0.72 M).

in the phosphate modified TiO₂ system suggests again that there are more organic intermediates generated during the oxidation of 4-CP.

As mentioned above, the hydroxyl radical is an important reactive species in the photocatalytic degradation. In our study, the formation of hydroxyl radical was examined by detecting the DMPO-OH adducts using EPR technique. The relative intensity changes of the EPR signals as a function of UV irradiation in the pure TiO₂ and phosphate modified TiO₂ dispersions are shown in Figure 8. In the pure TiO₂ system, the DMPO-OH adducts reached its maximum at 1 min and after that, the signal intensity underwent a gradual decrease with further irradiation time. The amount of DMPO-OH adducts in phosphate-modified TiO₂ system (TiO₂-P2) exhibited faster increase than that in the pure TiO₂ system, and no decrease was observed within 2 min of irradiation, which indicates that a much higher amount of •OH radical is produced in the phosphate modified system. It has been verified that DMPO-OH is relatively stable, with a half-life of about 20 min.^{34,37} The fast decrease (after 1 min of continuous irradiation) of the EPR signal intensity in the pure TiO₂ system can be ascribed to further oxidation of the adduct under photocatalytic conditions to form EPR-silent species. Dvoranova et al.³⁸ had assumed that the decrease of the EPR signal at longer irradiation times could result from the multiple addition of •OH to DMPO, or from the hole oxidation, or from the fast consumption of oxygen. In our study, the last possibility can be easily excluded considering that the samples for EPR detection were collected from stirring and aerating dispersions in the presence of DMPO and under UV irradiation. Conflicting with the assumption that the oxidation of DMPO-OH adduct is caused by the multiple attack of •OH on the DMPO, Hernandez-Alonso et al.³⁹ showed experimental evidence that the degradation of DMPO-OH radicals is derived from the direct oxidation by photogenerated holes. Therefore, the fast decrease of the EPR signal in the pure

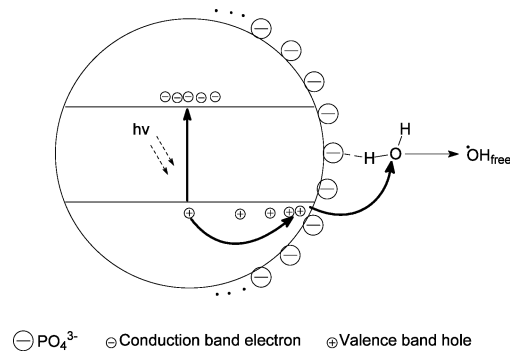
TiO₂ system and much more •OH radical detected upon phosphate modification again suggest that hole oxidation plays an important role in the former, whereas free •OH radical attack became predominant in the latter.

Mechanism Implication. The inorganic nonmetal anions, such as F⁻, PO₄³⁻, SO₄²⁻, and trifluoroacetic acid (TFA) have been reported to be effective modifiers to enhance the photocatalytic activity of TiO₂ catalyst.^{3,6–11,13,14} They have common characteristics, such as strong bonding ability on the surface of TiO₂, high negative-charge, easy formation of hydrogen bond, and chemical redox-inertness toward photogenerated electron and hole. We believe hence that the effects of modification by these inorganic nonmetal ions on the photocatalysis share the analogical mechanism. This argument can be further supported by the following facts: (1) The higher concentration of hydroxyl radical in the fluorinated TiO₂ system was also observed by Selli et al.,²² which is in consistent with the present study (Figure 8); (2) Both the phosphate anion⁴⁰ and fluoride anions⁶ can markedly shift the point of zero zeta potential (PZZP) of TiO₂ to a lower pH value, as measured by electrophoretic mobility; (3) Choi and co-workers⁶ found that both the adsorption and photodegradation rate of DCA markedly decreases in TiO₂-F system, and proposed that degradation on naked TiO₂ is initiated mostly by the direct hole transfer, whereas •OH radical play the role of a main oxidant in the F-TiO₂ system; (4) We also notice the existence of an induction period of TOC removal during the photocatalytic degradation of phenol in TiO₂-P2 and P0.10-TiO₂ similar to that in fluoride modified TiO₂ system; (5) Nearly all of the reported substrates with enhanced degradation in these anion-modified TiO₂ systems, such as phenol,^{3,6,9} Methylene blue,¹³ 4-nitrophenol,¹⁴ tetramethylammonium,⁷ and paraquat,⁴¹ have weak adsorption and tend to more probably undergo photodegradation by •OH radical attack pathway on pure TiO₂, which is similar to the phosphate modified system observed in this study (Figure 4).

Among the reports on the anion modification of TiO₂, only the operating mechanism of F-TiO₂ system has been considered intensively. In most of earlier studies, the enhancement of free •OH radical in F-TiO₂ system is only ascribed to inhibition of formation of adsorbed •OH radical by the replacement of OH_{ad} with F⁻,^{6,22} which can force the hole to react with the water to form free •OH radical. However, this proposition neglects the effect of anion adsorption on the energy band structure of TiO₂ semiconductor and on the hydrogen bond interaction between the anion and H₂O molecule. The present study would lay greater emphasis upon the importance of these effects on the photocatalytic process.

The above experimental results indicate that the effect of phosphate modification on the photocatalytic activity of TiO₂ is definitely attributed to the surface-bound phosphate anion. Further, the point of zero zeta potential (PZZP) of the TiO₂ particles are reported to be markedly shifted to lower pH value in the presence of phosphate anion,⁴⁰ indicating the accumulation of negative charges on the surface of TiO₂. It is apparent that the covering of the catalyst surface with negatively charged phosphate anions could form a negative electrostatic field in the surface layer of TiO₂. This negative electrostatic field can promote the separation of electrons and holes and suppress the charge recombination on phosphate modified TiO₂ compared with the pure TiO₂. As shown in Scheme 1, under ultraviolet irradiation, electron in the valence band in TiO₂ is excited to the conduction band to leave a positive hole in the valence band. The hole is drawn to the interface by the electrostatic force. However, the phosphate ions are known to have strong

SCHEME 1: Anion-Induced Negative Electrostatic Field and Electron-Transfer Pathway on the Phosphate Modified TiO₂ under UV Irradiation



interaction with H₂O through hydrogen bond, and the phosphate group has been proven to be a good anchor group to accomplish efficient electron transfer between the TiO₂ and chromophore in the photoelectron cell.^{42,43} All of these characteristics facilitate the charge transfer between the hole with H₂O to form free hydroxyl radicals. In addition, the replacement of OH_{ad} by phosphate can also inhibit the formation of surface-adsorbed hydroxyl radical. According to the proposed mechanism, both the surface hole and the free hydroxyl radical concentration might be enhanced after the phosphate modification. However, as mentioned above, the hole oxidation of substrates is more dependent on the adsorption of substrates than that of hydroxyl radical attack. In our study, the adsorption of nearly all of the substrates, especially for those with a strong adsorption on pure TiO₂ (such as DCA and AR), was suppressed upon phosphate modification. The suppression in adsorption could counteract the enhancement of hole concentration at the interface, while free hydroxyl radical can attack the substrates near the TiO₂ surface. As a result, the phosphate modification largely accelerates the hydroxyl oxidation pathway, but reduces the direct electron-transfer pathway. It should also be noted that the transfer of conduction band electron can also be possibly influenced by the phosphate modification and then may have some effects on the mineralization of organic compounds. This problem needs to be addressed further.

Conclusions

TiO₂ was modified by phosphoric anion before and after crystallization. It was found that the effect of phosphate modification is attributed to the surface-bound phosphate anion, rather than to the change in the crystallite structure or surface area (particle size) of TiO₂ by modification. The role of phosphate modification in the photocatalytic degradation of organic pollutants is two-edged: On one hand, it can inhibit the adsorption of most substrates, which tends to suppress their degradation, especially for the degradation of those substrates via the direct hole oxidation pathway. On the other hand, it can enhance the separation of photogenerated hole and electron by negative electrostatic field formed by the surface anion, and can force the formation of free hydroxyl radical. As a result, the effects of phosphate anion on the photocatalytic activity are very dependent on the kinds of substrates to be degraded. The degradation of substrates either susceptible to hydroxyl radical attack or with weak adsorption on the pure TiO₂ is significantly accelerated by phosphate modification through the hydroxyl radical attack pathway. However, the photodegradation of substrates, which is dominated through the hole oxidation pathway in the unmodified TiO₂ system (usually with strong

adsorption on the pure TiO₂), can be markedly suppressed by the hindered adsorption of substrates.

Acknowledgment. The generous financial support by the Ministry of Science and Technology of China (2007CB613306), by the National Science Foundation of China (20537010, 20520120221, and 50436040), and the Chinese Academy of Sciences is gratefully acknowledged.

Supporting Information Available: TGA curves; calculation formula for relative surface hydroxyl density; the FTIR spectra of P0.05-TiO₂, P0.10-TiO₂, P0.20-TiO₂; the Ti 2p and O 1s XPS spectra and the corresponding difference spectra of O 1s; the degradation kinetic curves of various of substrates and the degradation rates of hydroquinone. This material is available free of charge via the Internet at <http://pubs.acs.org>.

References and Notes

- (1) Linsebigler, A. L.; Lu, G.; Yates, J. T. *Chem. Rev.* **1995**, *95*, 735.
- (2) Ollis, D. F.; Al-Ekabi, H., Eds. *Photocatalytic Purification and Treatment of Water and Air*; Elsevier: Amsterdam, 1993.
- (3) Minero, C.; Mariella, G.; Maurino, V.; Pelizzetti, E. *Langmuir* **2000**, *16*, 2632.
- (4) Hoffmann, M. R.; Martin, S. T.; Choi, W.; Bahnemann, D. W. *Chem. Rev.* **1995**, *95*, 69.
- (5) Kesselman, J. M.; Weres, O.; Lewis, N. S.; Hoffmann, M. R. *J. Phys. Chem. B* **1997**, *101*, 2637.
- (6) Park, H.; Choi, W. *J. Phys. Chem. B* **2004**, *108*, 4086.
- (7) Vohra, M. S.; Kim, S.; Choi, W. *J. Photochem. Photobiol., A* **2003**, *160*, 55.
- (8) Minero, C.; Mariella, G.; Maurino, V.; Vione, D.; Pelizzetti, E. *Langmuir* **2000**, *16*, 8964.
- (9) Korosi, L.; Dekany, I. *Colloid Surf. A-Physicochem. Eng. Asp.* **2006**, *280*, 146.
- (10) Korosi, L.; Papp, S.; Bertoti, I.; Dekany, I. *Chem. Mater.* **2007**, *19*, 4811.
- (11) Yu, J. C.; Zhang, L.; Zheng, Z.; Zhao, J. *Chem. Mater.* **2003**, *15*, 2280.
- (12) Lin, L.; Lin, W.; Xie, J. L.; Zhu, Y. X.; Zhao, B. Y.; Xie, Y. C. *Appl. Catal., B* **2007**, *75*, 52.
- (13) Mohapatra, P.; Parida, K. M. *J. Mol. Catal., A* **2006**, *258*, 118.
- (14) Samantaray, S. K.; Mohapatra, P.; Parida, K. *J. Mol. Catal., A* **2003**, *198*, 277.
- (15) Yu, J. C.; Ho, W.; Yu, J.; Hark, S. K.; Iu, K. *Langmuir* **2003**, *19*, 3889.
- (16) Connor, P. A.; McQuillan, A. J. *Langmuir* **1999**, *15*, 2916.
- (17) Huang, L.; Li, Q. *Chem. Lett.* **1999**, 829.
- (18) Ciesla, U.; Schacht, S.; Stucky, G. D.; Unger, K. K.; Schuth, F. *Angew. Chem., Int. Ed. Engl.* **1996**, *35*, 541.
- (19) Abdullah, M.; Low, G. K. C.; Matthews, R. W. *J. Phys. Chem.* **1990**, *94*, 6820.
- (20) Li, X.; Cabbage, J. W.; Tetzlaff, T. A.; Jenks, W. S. *J. Org. Chem.* **1999**, *64*, 8509.
- (21) Li, X.; Cabbage, J. W.; Jenks, W. S. *J. Org. Chem.* **1999**, *64*, 8525.
- (22) Mrowetz, M.; Selli, E. *Phys. Chem. Chem. Phys.* **2005**, *7*, 1100.
- (23) Mueller, R.; Kammler, H. K.; Wegner, K.; Pratsinis, S. E. *Langmuir* **2003**, *19*, 160.
- (24) Zhu, J.; Yang, J.; Bian, Z.-F.; Ren, J.; Liu, Y.-M.; Cao, Y.; Li, H.-X.; He, H.-Y.; Fan, K.-N. *Appl. Catal., B* **2007**, *76*, 82.
- (25) Nagaveni, K.; Hegde, M. S.; Ravishankar, N.; Subbanna, G. N.; Madras, G. *Langmuir* **2004**, *20*, 2900.
- (26) Baunack, S.; Oswald, S.; Scharnweber, D. *Surf. Interface Anal.* **1998**, *26*, 471.
- (27) Alfaya, A. A. S.; Gushikem, Y.; de Castro, S. C. *Chem. Mater.* **1998**, *10*, 909.
- (28) Sodergren, S.; Siegbahn, H.; Rensmo, H.; Lindstrom, H.; Hagfeldt, A.; Lindquist, S. E. *J. Phys. Chem. B* **1997**, *101*, 3087.
- (29) Weng, Y. X.; Li, L.; Liu, Y.; Wang, L.; Yang, G. Z. *J. Phys. Chem. B* **2003**, *107*, 4356.
- (30) Huber, R.; Moser, J. E.; Gratzel, M.; Wachtveitl, J. *J. Phys. Chem. B* **2002**, *106*, 6494.
- (31) Stafford, U.; Gray, K. A.; Kamat, P. V. *J. Phys. Chem.* **1994**, *98*, 6343.
- (32) Theurich, J.; Lindner, M.; Bahnemann, D. W. *Langmuir* **1996**, *12*, 6368.
- (33) Chen, C.; Lei, P.; Ji, H.; Ma, W.; Zhao, J.; Hidaka, H.; Serpone, N. *Environ. Sci. Technol.* **2004**, *38*, 329.
- (34) Grela, M. A.; Coronel, M. E. J.; Colussi, A. J. *J. Phys. Chem.* **1996**, *100*, 16940.
- (35) Li, X.; Jenks, W. S. *J. Am. Chem. Soc.* **2000**, *122*, 11864.
- (36) Cermenati, L.; Pichat, P.; Guillard, C.; Albini, A. *J. Phys. Chem. B* **1997**, *101*, 2650.
- (37) Krishna, V.; Yanes, D.; Imaram, W.; Angerhofer, A.; Koopman, B.; Moudgil, B. *Appl. Catal., B* **2007**, in press.
- (38) Dvoranová, D.; Brezová, V.; Mazúr, M.; Malatí, M. A. *Appl. Catal., B* **2002**, *37*, 91.
- (39) Hernández-Alonso, M. D.; Hungría, A. B.; Martínez-Arias, A.; Fernández-García, M.; Coronado, J. M.; Conesa, J. C.; Soria, J. *Appl. Catal., B* **2004**, *50*, 167.
- (40) Nelson, B. P.; Candal, R.; Corn, R. M.; Anderson, M. A. *Langmuir* **2000**, *16*, 6094.
- (41) Vohra, M. S.; Tanaka, K. *Environ. Sci. Technol.* **2001**, *35*, 411.
- (42) Bae, E.; Choi, W.; Park, J.; Shin, H. S.; Kim, S. B.; Lee, J. S. *J. Phys. Chem. B* **2004**, *108*, 14093.
- (43) Ernstorfer, R.; Gundlach, L.; Felber, S.; Storck, W.; Eichberger, R.; Willig, F. *J. Phys. Chem. B* **2006**, *110*, 25383.